Spring 4-2014

Synthesis and Characterization of Three Unique Mono-Metallic Lanthanide Complexes

Jasminder S. Grewal

Synthesis and Characterization of Three Unique Mono-Metallic Lanthanide Complexes

Honors Thesis

Jasminder S. Grewal

Department: Chemistry

Advisor: Shawn Swavey, Ph.D.

April 2014

Synthesis and Characterization of Three Unique Mono-Metallic Lanthanide Complexes

Honors Thesis

Jasminder S. Grewal

Department: Chemistry

Advisor: Shawn Swavey, Ph.D.

April 2014

Abstract

Three unique lanthanide complexes of formula $Ln(tdh)_3dpp$ (where Ln = Eu^{3+}, Tb^{3+}or Nd^{3+}; tdh = 1,1,1-trifluoro-5,5-dimethyl-2,4-hexanedione and dpp = 2,3-Bis(2-pyridyl)pyrazine) were structurally characterized. X-ray quality crystals were grown through slow evaporation in a solution of concentrated ethyl acetate and hexanes. Each of the metals are eight coordinate, with 6 oxygen atoms from the tdh ligand and two nitrogen atoms from the dpp. Specifically, the nitrogen from 1-pyridyl group and the 1-pyrazine group coordinate to the lanthanide metal. Luminescent studies were performed on all three compounds. The Eu and Tb complexes were able to emit light in the visible region of the spectrum when the solutions are excited at 288 nm, which causes the π-π* transition to occur in the tdh ligand. Emission lines corresponding to transitions from the $^5D_0$ and $^5D_4$ state to the ^7F_J manifold of the Eu(III) and Tb(III), respectively, are observed. The intensity of these emissions increases as the temperature is decreased.

Dedication or Acknowledgements

I would like to thank Dr. Shawn Swavey for all of the support that he has given me throughout this process. I would like thank my family, friends, the Chemistry Department and my fellow chemistry majors for the support throughout the years.

UNIVERSITY of DAYTON

Table of Contents

Abstract	Title Page
Introduction	1
Experimental	4
Results and Discussion	7
Conclusion	14
References	15
Appendix	17

1. Introduction

The lanthanide series consist of the lanthanide metals. The term originates from the first lanthanide metal, called Lanthanum, which has an atomic number of 57. They can react with water at cold temperatures but the reaction can be further accelerated if there is heat present. These metals have become widely studied because of their luminescent properties. They have long excited state lifetimes and narrow emission lines making them ideal components in equipment such as fluorescent tubes, electroluminescent devices, photo catalysts [1], solid state lasers [2, 3], optical fibers [4-6], biomedical assays [7], immunoassays [8], early detection of cancer, [9] and in time resolved luminescence measurements [10]. The most stable form of the lanthanide metals is the 3+ oxidation state [10]. The electronic configuration for lanthanides is as follows: $1s^2 2s^2 2p^6 3s^2 3p^6 4s^2 3d^{10} 4p^6 5s^2 4d^{10} 5p^6 6s^2 4f^n$, where n stands for the number of electrons in the 4f orbital. These 4f orbitals can be excited to the 4f* orbitals. This is known as the HOMO, highest occupied molecular orbital, to LUMO, lowest unoccupied molecular orbital, transition. When an electron gets excited, it needs to receive enough energy in order to reach the excited state from its ground state. When an electron falls from the excited state to the ground state, it may release a photon of energy. This photon of energy provides details about the energy gap between the HOMO and LUMO energy states. The 4f-4f* transition in lanthanide complexes is symmetry forbidden and therefore researchers have sought other ways to access these excited states.

Beta-diketones (β-diketones) are used to access the 4f* orbitals of the lanthanide metals. β-diketones typically have two coordination sites on the compound that can

coordinate to the lanthanide metals. These ligands are there known as bidentate ligands, due to this property. One advantage of using these ligands is that it allows access to excited states of the lanthanide metals. Quantum mechanics states the 4f-4f* transition in lanthanides are Laporte forbidden and cannot be accessed by shining light directly but, β-diketones are used to access these excited states [11, 12], because of this these ligands are referred to as “antenna” ligands. Temperature dependent luminescence is a characteristic of lanthanide complexes that contain these ligands. These complexes are used as temperature probes [13, 14] because of the effects of temperature on their luminescent properties.

In addition to β-diketonates researchers have found utility in coordinating polypyridyl ligands to lanthanides[10]. One advantage of attaching polypyridyl ligands is enhancement of the luminescent properties of the complexes [15]. They have also been used to determine the magnetic interactions that occur between metal centers as a model for larger complexes [15]. One class of polypyridyl ligands commonly used are bridging ligands which allow for coordination of two lanthanide metal centers. For example, the bridging ligand in the complexes study in this work is called 2,3-Bis(2-pyridyl)pyrazine (dpp). This has 4 nitrogen atoms on the structure (2 on each side as seen in Figure 1 below) that allow for coordination of two metal centers. Figure 1 shows that two of the nitrogen atoms have been used up to coordinate with the lanthanide metal, which leaves two nitrogen atoms to coordinate to another metal atom. The other commonly used bridging ligand in Figure 1 is 2, 2’ – bipyrimidine (bpm) [12].

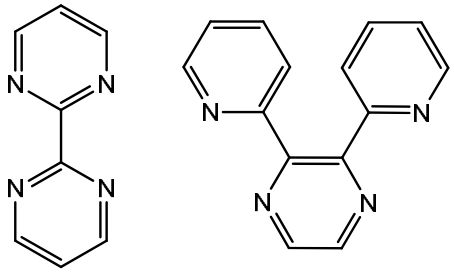

Figure 1. Examples of bridging ligands.

This project involved the use of three lanthanide metals (Nd (III), Eu (III), and Tb(III)). The β-diketone, 1,1,1-trifluoro-5,5-dimethyl-2,4-hexanedione (tdh), and the bridging ligand, 2,3-Bis(2-pyridyl)pyrazine (dpp), to synthesize three new monometallic lanthanide complexes. The complexes were characterized by X-ray crystallography and elemental analysis. Temperature dependent luminescent studies were also performed.

2. Experimental

2.1 Materials

Any of the reagents that were used in the experiment were analytical grade and used without further purification. Europium(III) chloride (Acros Organics), terbium(III) chloride (Acros Organics), neodymium(III) chloride (Acros Organics). 2,3-Bis(2-pyridyl)pyrazine (Aldrich), 1,1,1-trifluoro-5,5-dimethyl-2,4-hexanedione (Acros Organics), sodium hydroxide (Fischer), ethanol (Decan), ethyl acetate, hexanes (Fischer), and methanol (Fischer) were used as they were received. The elemental analysis was by Atlantic Microlabs Inc., Norcross, Georgia.

2.2 Synthesis

The same general procedure was used for all three complexes differing only in the quantities of starting materials used. For example, 2.73 mmoles of the lanthanide (III) chloride salt in 10 mL of deionized water was added to a 15 mL solution of ethanol containing 2.75 mmoles of dpp in 15 mL of ethanol in a 50 mL round bottom flask. The reaction mixture was refluxed for 30 min. In a separate flask 8.19 mmoles of tdh and 8.2 mmoles of NaOH were dissolved in 15 mL of ethanol and allowed to stir at room temperature for 30 min. The tdh solution was added to the refluxing lanthanide(III)/dpp solution and the solution was brought to room temperature. After ca. 30 min. stirring at room temperature a precipitate formed which was filtered and recrystallized in an ethyl acetate/hexane solution.

$Eu(tdh)_3dpp$ (1): Yield 0.866 g (85.5%) F.W. (971.74) Anal. Calc. for $C_{38}H_{40}N_4O_6F_9Eu \cdot H_2O$: C, 46.11; H, 4.28; N, 5.66; F, 17.28. Found: C, 46.40; H, 4.17; N, 5.71; F, 16.96.

Tb(tdh)$_3$dpp (2): Yield 0.483 g (96.5%) F.W. (979.54) Anal. Calc. for $C_{38}H_{40}N_4O_6F_9Tb$: C, 46.64; H, 4.12; N, 5.73; F, 17.47. Found: C, 46.28; H, 4.11; N, 5.69; F, 17.10.

Nd(tdh)$_3$dpp (3): Yield 0.669 g (91.5%) F.W. (963.94) Anal. Calc. for $C_{38}H_{40}N_4O_6F_9Nd$: C, 47.34; H, 4.18; N, 5.81; F, 17.74. Found: C, 47.55; H, 4.11; N, 5.89; F, 17.57.

2.3 Physical Measurements

UV/Vis spectra were recorded at room temperature using a Schimadzu 1501 photodiode array spectrophotometer with 2 nm resolution. Samples were run in reagent-grade methanol in 1 cm quartz cuvettes. Luminescence spectra of the europium and terbium complexes in 1 cm quartz fluorometer cells in methanol were run on a Cary Eclipse fluorescence spectrophotometer. Temperature dependent luminescence of the europium and terbium complexes in methanol from 10 °C to 50 °C was controlled using a Cary single cell peltier temperature controller.

A colorless crystal of **1** having approximate dimensions 0.1985 mm x 0.1335 mm x 0.0804 mm was used for X-ray crystallographic analysis. The X-ray intensity was measured at 110 K on an Oxford Diffraction Xcaliber3 system equipped with a Sapphire3 and an Enhance (Cu) source (λ=1.54180 Å) operated at 40 mA and 40 kV. Final cell constants were obtained through a global refinement of all reflections. Intensity data were collected using ω scans employing the *CrsyAlis CCD*. WinGX was used to label the structure and provide one for refinement. The structure was solved and refined using Bruker SHELXTL (v6.10). Crystal data can be found in Table 2 in the Appendix.

A colorless crystal of **2** having approximate dimensions 0.2833 mm x 0.1007 mm x 0.0762 mm was used for the X-ray crystallographic analysis. The X-ray intensity was measured at 110 K on an Oxford Diffraction Xcaliber3 system equipped with a Sapphire3

and an Enhance (Cu) source (λ=1.54180 Å) operated at 40mA and 40kV. Final cell constants were obtained through a global refinement of all reflections. Intensity data were collected using ω scans employing the *CrsyAlis CCD*. WinGX was used to label the structure and provide one for refinement. The structure was solved and refined using Bruker SHELXTL (v6.10). Crystal data can be found in Table 2 in the Appendix.

A purple crystal of **3** having approximate dimensions 0.2552 mm x 0.2338 mm x 0.1047 mm was used for X-ray crystallographic analysis. The X-ray intensity was measured at 110 K on an Oxford Diffraction Xcaliber3 system equipped with a Sapphire3 and an Enhance (Cu) source (λ=1.54180 Å) operated at 40mA and 40kV. Final cell constants were obtained through a global refinement of all reflections. Intensity data were collected using ω scans employing the *CrsyAlis CCD*. WinGX was used to label the structure and provide one for refinement. The structure was solved and refined using Bruker SHELXTL (v6.10). Crystal data can be found in Table 2 in the Appendix.

3. Results and Discussion

3.1 Synthesis and Structural Analysis

The synthesis of the complexes was performed using the β-diketone, tdh. This was converted from its original β-diketone form to the enolate form by a reaction with the base, sodium hydroxide. Then, in a 1:1 equivalent ratio, the lanthanide salt was refluxed with dpp in the presence of ethanol for 30 minutes. The enolate form of the tdh was added to the mixture, as shown in Figure 2. After the compound was cooled to room temperature, a precipitate was filtered and recrsytallized using a mixture of ethyl acetate and hexanes. The resulting yield was larger than 80% for each of the $Ln(tdh)_3dpp$ complexes.

X-ray diffraction quality crystals were grown by allowing for a slow evaporation of concentrated ethyl acetate solutions. Each of the complexes crystallized without solvent in a triclinic space group P-1. Space groups depict the symmetry of a crystal in three-dimensional space. Each of the three lanthanide centers is eight coordinate and the complexes are neutral. Eight coordinate means that there are eight atoms that are attached to the lanthanide metal. Of the eight atoms, 6 are oxygen atoms and the other two are nitrogen atoms. The oxygen atoms come from the tdh antenna ligand and the nitrogen atoms come from the dpp bridging ligand. In Table 1 below indicates the bond lengths between each of the lanthanide metals and the eight atoms that are coordinated to them.

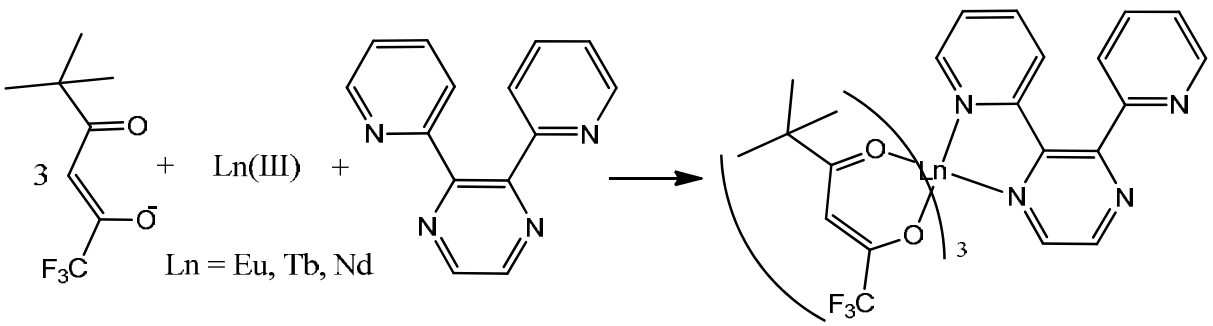

Figure 2. Scheme for the formation of the lanthanide complexes

Table 1. Selected Bond Lengths (Å) for Nd(III), Tb(III) and Eu(III) complexes.

Nd		Tb		Eu	
Nd-O1	2.357(3)	Tb -O1	2.338(3)	Eu -O1	2.378(3)
Nd-O5	2.399(3)	Tb -O2	2.325(3)	Eu -O5	2.337(3)
Nd-O2	2.443(3)	Tb -O5	2.350(3)	Eu -O3	2.323(3)
Nd-O3	2.387(3)	Tb -O4	2.383(3)	Eu -O4	2.343(3)
Nd-O4	2.411(3)	Tb -O6	2.320(3)	Eu -O6	2.327(3)
Nd-O6	2.389(3)	Tb -O3	2.298(3)	Eu -O2	2.299(3)
Nd-N1	2.617(4)	Tb -N1	2.546(3)	Eu -N1	2.548(3)
Nd-N2	2.678(4)	Tb –N2	2.595(4)	Eu -N2	2.591(3)

Figure 3-5 depict the eight coordinate structure of each of the complexes. In Figure 3, the Nd(III) ion is in a distorted square-antiprismatic geometry with the approximate square planes defined as Nd1-O5–O6–C32- C31-C37 and Nd1-N1-N2–C5–C6 (mean deviation of 0.0296 Å

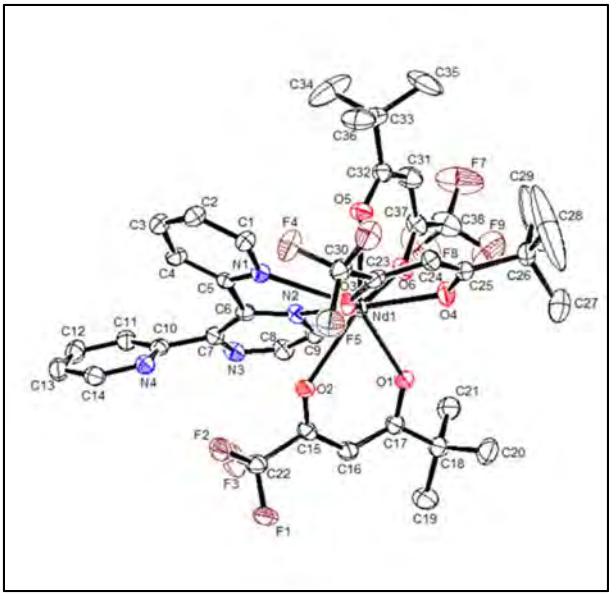

Figure 3. Molecular structure of Nd(tdh)$_3$dpp showing atomic numbering scheme, 50% thermal ellipsoid probability, H-atoms omitted for clarity.

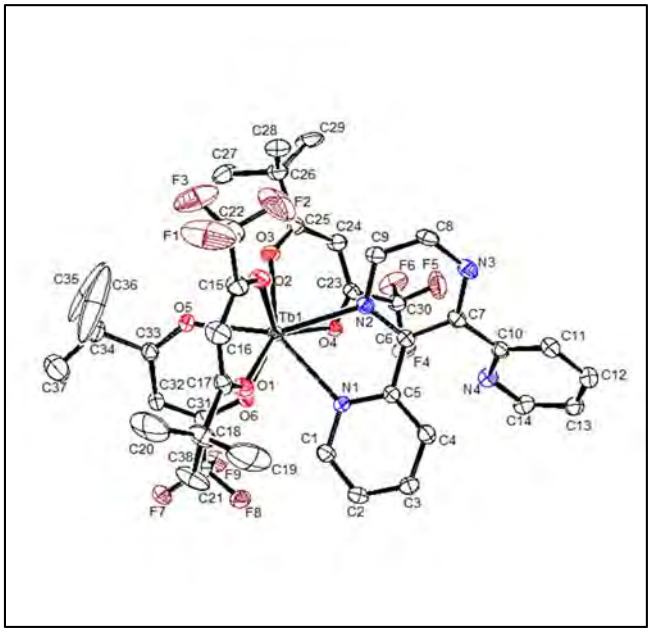

Figure 4. Molecular structure of Tb(tdh)$_3$dpp showing atomic numbering scheme, 50% thermal ellipsoid probability, H-atoms omitted for clarity.

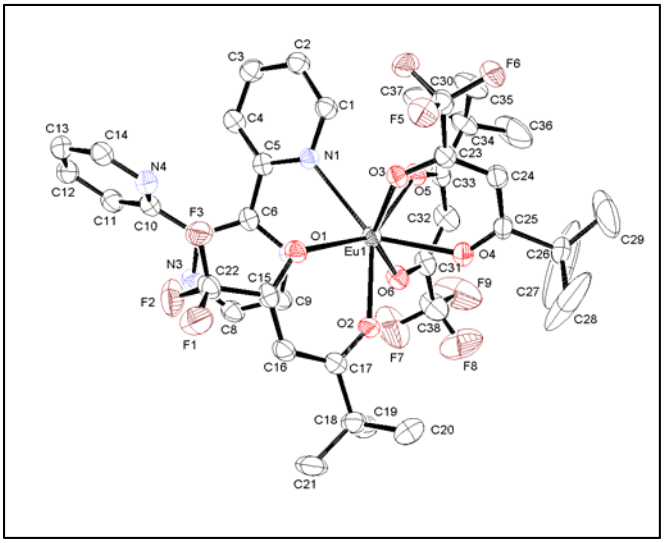

Figure 5. Molecular structure of Eu(tdh)$_3$dpp showing atomic numbering scheme, 50% thermal ellipsoid probability, H-atoms omitted for clarity.

and 0.0970 Å, respectively), with an angle between the planes of 95.6°. The corresponding planes for the Tb complex (Figure 4) are: Tb1-O1-O2-C15-C16-C17 and Tb1-N1-C5-C6-N2 with respective mean deviations of 0.0317 Å and 0.0944 Å; and for the Eu complex (Figure 5) the corresponding planes and deviations are: Eu1-O5-O6-C31-C32-C33 (0.0351 Å) and Eu1-N1-C5-C6-N2 (0.0928 Å) with dihedral angle of 96.9°. The dpp ligand contains freely rotating pyridyl groups which are oriented so as to relieve any close hydrogen–hydrogen atom repulsions, in contrast to the close hydrogen-hydrogen H4A …H11A repulsions (2.947 Å) observed in previous complexes [16]. The two dihedral angles between pyrazine and pyridyl mean planes average 25.8° and 42.6°.

3.2 Temperature dependent luminescence

Temperature dependent luminescent studies were performed on methanol solutions of the Eu(III) and Tb(III) complexes. No emission was detected for a methanol solution of the Nd(III) complex in the range 350 nm to 1100 nm when irradiated at 288 nm. The low energy excited states of Nd(III) complexes have been noted to undergo

rapid vibrational deactivation through solvent interactions [17].

The electronic spectra of all complexes is dominated by π-π* transitions of the tdh ligands with a peak absorption occurring at 288 nm. The emission and temperature dependent spectra of $Eu(tdh)_3dpp$ in methanol is illustrated in Figure 6. The ground state electronic configuration for

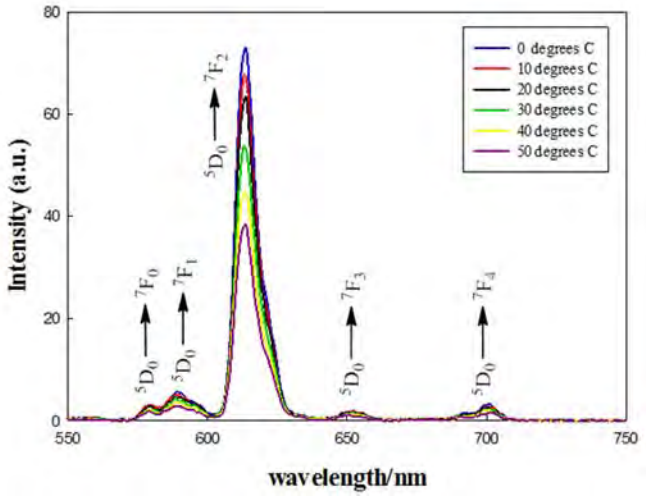

Figure 6. Luminescent and temperature dependent emission spectra of a methanol solution of $Eu(tdh)_3dpp$ in the temperature range of 5 ºC to 40 ºC, λ_{exc} = 288 nm.

Eu(III) is $[Xe]4f^6$ with free ion ground term ^7F_J and spin-orbit coupling values (J = 0, 1, 2, 3, 4, 5, 6). Upon excitation of the π-π* transitions of the tdh ligand from S_0-S_1 intersystem crossing to the triplet state T_1 occurs followed by rapid conversion from T_1 to $^5D_0$ state of the Eu(III) center. Relaxation from the $^5D_0$ state to the ^7F_J manifold results in the luminescent peaks observed in Figure 4, with the most intense peak at 614 nm corresponding to the $^5D_0$ to $^7F_2$ transition. We were unable to observe transitions from $^5D_0$ to the $^7F_5$ and $^7F_6$ states presumably due to their comparative low intensities. As the temperature of the solution is increased the intensity of the emissions decreases due to thermal population of the T_1 state of the tdh ligand from the $^5D_0$ state of the Eu(III) [18].

The electronic configuration of the Tb(III) ion is [Xe]$4f^8$ with free ion ground term ^7F_J and spin-orbit coupling values in decreasing order of energy (J = 6, 5, 4, 3, 2, 1, 0) due to the more than half filled nature of the f-orbitals according to Hund's third rule. Upon excitation of the tdh ligand at 288 nm from S_0 to S_1 a similar intersystem crossing occurs to the T_1 state followed by transfer to the excited $^5D_4$ state of Tb(III), leading to the emission spectrum illustrated in Figure 7. The most intense emission is observed at ca. 550 nm associated with the $^5D_4$ to $^7F_5$ transition. Due to low intensity the $^5D_4$ to $^7F_1$ and $^7F_0$ states are not observed. For similar reasons as those observed for the Eu(tdh)$_3$dpp complex the intensity of the emission spectra decreases as the temperature of the Tb(tdh)$_3$dpp solution is increased.

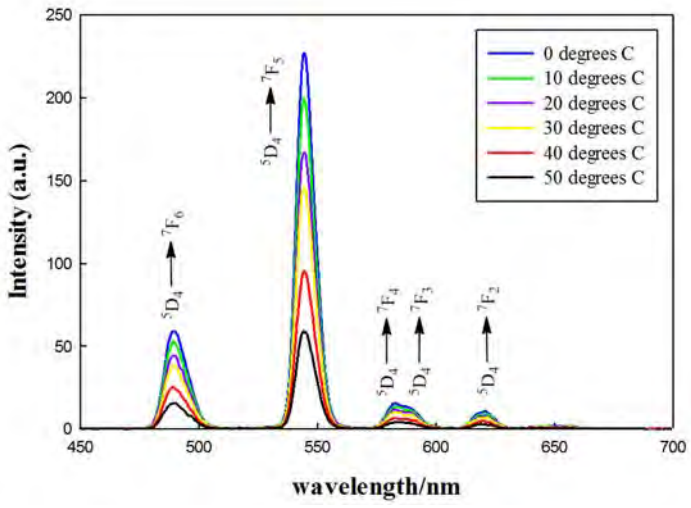

Figure 7. Luminescent and temperature dependent emission spectra of a methanol solution of Tb(tdh)$_3$dpp in the temperature range of 5 ºC to 40 ºC, λ_{exc} = 288 nm.

It is interesting to note that the emission spectra observed for the monometallic Tb(III) and Eu(III) complexes presented here are considerably sharper and more well defined than the homodinuclear Eu(III) and Tb(III) complexes studied in this laboratory.

This may suggest a type of electronic communication or possible quenching in the bimetallic complexes.

4. Conclusion

In conclusion, three new mono-metallic Eu(III), Tb(III), and Nd(III) complexes containing dpp were synthesized in high yield. The lanthanides of each complex are eight coordinate from six oxygen atoms of the tdh ligands and two nitrogen atoms of the dpp. Each of the complexes crystallize into a triclinic P-1 space group. Luminescent properties of the Eu(III) and Tb(III) complexes in methanol solutions show sharp emission lines from the excited f-orbitals to the ^7F_J manifold. Increasing temperature of the solutions decreases the emission intensity due to repopulation of the T_1 state of the tdh ligands. Further studies, that are currently underway, are trying to attach Ru(II) polypyridyl groups to the free nitrogens on the dpp bridging ligand.

5. References

[1] B. Marciniak, G.L. Hug, Coord. Chem. Rev. 159 (1997) 55; Z. Xu, Q. Yang, C. Xie, W. Yan, Y. Du, Z. Gao, J. Zhang, J. Mat. Sc. 40 (2005) 1539

[2] X.L. Ji, B. Li, S. Jiang, D. Dong, H.J. Zhang, X.B. Jing, B.Z. Jiang, J. Non-Crsyt. Solids 52 (2000) 275.

[3] R.F deFarias, S. Alves, Jr., M.F. Belian, G.F. deSa, Opt. Mater. 26 (2004) 199.

[4] J. Sokolnicki, R. Wiglusz, S. Radzki, A. Graczyk, J. Legendziewicz, Opt. Mater. 26 (2004) 199.

[5] A.K. Kewell, G.T. Reed, F. Namavar, Sens. Actuators, A 65 (1998) 160.

[6] P.C. Russell, R. Haber, G.R. Jones, W. McGrory, Sens. Actuators, A 76 (1991) 231.

[7] H.V. Martinus, R.H. Woudenberg, P.G. Emmerink, R. vanGassel, J.H. Hofstraat, J.W. Vernhoeven, Angew. Chem. Int. Ed. 39 (2000) 4542.

[8] S. Liu, Chem. Soc. Rev. 33 (2004) 445

[9] I. Billard, in: K.A. Gschneidner Jr., al. et (Eds.), Handbook on the Physics and Chemistry of Rare Earths, col. 33, Elsevier Science, Amsterdam, 2003, p. 465

[10] S.Swavey, R.Swavey, Coord. Chem. Rev. (2009), doi: 10.1016/j.ccr.2009.05.015

[11] F.S. Richardson, Chem. Rev. 82 (1982) 541.

[12] S. Swavey, J.A. Krause, D. Collins, D. D'Cunha, A. Frantini, *Polyhedron.* 2008, 27, 1061-1069

[13] S.M. Borisov, O.S. Wolfbeis, Anal. Chem. 78 (2006) 5094

[14] Y. Liu, G. Qian, Z. Wang, M. Wang, Appl. Phy. Let. 86 (20058) 071907/1

[15] (a) S. Pandya, J. Yu, D. Parker, Dalton Trans. (2006) 2757
(b) S. Aime, S. Geninatti Crich, E. Gianolio, G.B. Giovenzana, L. Tei, E. Terreno, Coord. CHem. Rev. 250 (2006) 1562

[16] S. Viviani, A. Fratini, S. Swavey, *Inorg. Chem. Commun*. 2012, 24, 29-31.

[17] S. Biju, M.L.P. Reddy, R.O. Freire, *Inorg. Chem. Commun*. 2007, 10, 393-395.

[18] N.M. Shavaleev, S.J.A. Pope, Z.R. Bell, S. Faulkner, M.S. Ward, *Dalton Trans*. 2003, 808-814.

6. Appendix

Table 2. Crystal Data and Structure Refinement Parameters for Complexes Nd(III), Tb(III) and Eu(III).

Parameters	**Nd**	**Tb**	**Eu**
empirical formula	$C_{38}H_{40}N_4O_6F_9Nd$	$C_{38}H_{40}N_4O_6F_9Tb$	$C_{38}H_{40}N_6O_7F_{18}Eu$
fw	963.98	978.66	971.70
crystal system	Triclinic	Triclinic	Triclinic
space group	P-1	P-1	P-1
cryst. size (mm^3)	0.105x0.234x0.255	0.076x0.101x0.283	0.080x0.134x0.199
temperature (K)	110	110	110
a(Å)	10.0573(4)	10.0672(3)	10.0675(4)
b(Å)	12.6204(8)	12.5415(6)	12.5330(6)
c(Å)	17.8306(7)	17.8403(8)	17.8656(6)
α(°)	91.755(4)	91.595(4)	91.574(3)
β(°)	95.234(5)	95.606(3)	95.636(3)
γ(°)	112.878(5)	113.304(4)	113.368(4)
V($Å^3$)	2071.07(17)	2053.37(15)	2053.86(15)
Z	2	2	2
$_{calc}$(g cm^{-3})	1.546	1.583	1.571
μ(mm^{-1})	10.356	9.267	11.728
R1[I>2σ(I)]	0.0408	0.0389	0.0405
wR2[I>2σ(I)]	0.0954	0.0916	0.0948
R1(all data)	0.0466	0.0435	0.0454
wR2(all data)	0.1011	0.0952	0.0986
GOF	1.010	1.025	1.026
refl.measured/ independent refl.	14018/7038	12040/6760	12228/6982
max \º	65.08º	63.68º	65.08º